Calibrating Focal Length for Paracatadioptric Camera from One Circle Image

Huixian Duan, Lin Mei, Yanfeng Shang and Chuanping Hu
R & D Center of Cyber-Physical Systems, The Third Research Institute of Ministry of Public Security, Bisheng Road, Shanghai, China

Keywords: Focal Length, Calibration, Paracatadioptric Camera, Circle Image.

Abstract: Camera calibration from circles has great advantages, but for paracatadioptric camera, the estimation of intrinsic parameters using circle images is still an open and challenging problem. Previous work proved that the paracatadioptric projection of a circle is a quartic curve. But due to the partial occlusion, only part of the quartic curve is visible on the image plane. Consequently, circle image cannot be directly estimated using image points extracted from the visible part and camera parameters cannot be calibrated. To solve this problem, In this paper, we study the properties of paracatadioptric circle image and application in calibrating the focal length for the case that aspect ratio is 1 and skew is 0. Firstly, we derive the necessary and sufficient conditions that must be satisfied by paracatadioptric circle image. Next, based on these conditions, a new object function is presented to correctly estimate the circle image. Then, we show that the focal length can be computed from the estimated paracatadioptric circle image and the principal point that is estimated from the projected contour of parabolic mirror. Experimental results on both simulated and real image data have demonstrated the effectiveness of our method.

1 INTRODUCTION

Many applications in computer vision require that a camera has a large field of view. Combining the camera with mirrors, referred to as catadioptric image formation, can increase the field of view of a camera. According to the uniqueness of an effective viewpoint, catadioptric systems can be classified into two groups, central and noncentral (Baker and Nayer, 1999). Baker and Nayer (Baker and Nayer, 1999) introduced that a central catadioptric system can be built by combining an hyperbolic mirror with a perspective camera, a parabolic mirror with an orthographic camera, and planar mirror with a perspective camera. The construction of the former requires a careful alignment between the mirror and the imaging device. But the paracatadioptric camera is easier to construct being broadly used in vision applications.

Geyer and Daniilidis (Geyer and Daniilidis, 2001) proposed a unifying model for general central catadioptric image formation. It is shown that the imaging process is equivalent to the two-step mapping by a sphere. Under central catadioptric system, the calibration of camera is still a prerequisite for its applications. In the literature, the calibration methods can be classified into the following four categories. The first category (Aliaga, 2001; Wu and Hu, 2005; Scaramuzza et al., 2006; Deng et al., 2007; Bastanlar et al., 2008) require a 3D/2D calibration pattern with control points. The second category (Geyer and Daniilidis, 1999; Geyer and Daniilidis, 2002; Barreto and Araujo, 2002; Barreto and Araujo, 2003; Barreto and Araujo, 2005; Barreto and Araujo, 2006; Geyer and Daniilidis, 2002; Wu et al., 2006; Scaramuzza et al., 2006; Wu et al., 2008; Duan et al., 2012) only make use of the properties of line images. The third category (Ying and Hu, 2004; Ying and Zha, 2008; Duan and Wu, 2011a; Duan and Wu, 2012)is based on the properties of sphere images. The fourth category (Kang, 2000) only use point correspondence in multiple views, without needing to know either the 3D location of space points or camera locations.

Camera calibration from circles has great advantages. Especially, as a kind of central catadioptric cameras, there have been many calibration methods of the pinhole camera based on circle images in the literature, and these methods can get high calibration accuracy. However, due to large distortion, catadioptric camera calibration from circle images has many difficulties and lacks of studies. Based on the projection of a line complex, Sturm and Barreto(Sturm and Barreto, 2008) proved that the central catadiop-

Duan H., Mei L., Shang Y. and Hu C..
Calibrating Focal Length for Paracatadioptric Camera from One Circle Image.
DOI: 10.5220/0004672800560063
In *Proceedings of the 9th International Conference on Computer Vision Theory and Applications* (VISAPP-2014), pages 56-63
ISBN: 978-989-758-003-1

tric projection of a quadric is a quartic curve. What's more, according to the imaging process under central catadioptric model, Duan and Wu (Duan and Wu, 2011b) derived the algebraic expression of a circle image and provided a unified imaging theory of different geometric elements, which established the theoretical foundation for calibration methods based on circles. But due to the partial occlusion, only part of the circle image is visible on the image plane. Consequently, circle image cannot be directly estimated using image points extracting from the visible part and camera parameters cannot be calibrated.

In this paper, for the case that aspect ratio is 1 and skew is 0, we study the properties of paracatadioptric circle image and application in calibrating the focal length. Firstly, the necessary and sufficient conditions that must be satisfied by paracatadioptric circle image are derived. Secondly, these conditions are used to correctly estimate the paracatadioptric circle image. Finally, we show that the focal length can be calibrated from the estimated paracatadioptric circle image and the principal point that is estimated from the projected contour of parabolic mirror. Experimental results on both simulated and real image data have demonstrated the effectiveness of our method.

This paper is organized as follows: Section 2 reviews the unified sphere model introduced by Geyer and Daniilidis (Geyer and Daniilidis, 2001) and some related works. Section 3 studies the properties of paracatadioptric circle image. In section 4, the focal length is calibrated from one circle image and the principal point. Experimental results are shown in Section 5. Finally, Section 6 presents some concluding remarks.

2 PRELIMINARIES

A bold letter denotes a vector or a matrix. Without special explanation, a vector is homogenous coordinates. In the following, we briefly review the image formation for paracatadioptric camera introduced in (Geyer and Daniilidis, 2001), the antipodal image points and their properties proposed in (Wu et al., 2008) and the algebraic expression of paracatadioptric circle image derived in (Duan and Wu, 2011b).

2.1 Paracatadioptric Projection Model

Geyer and Daniilidis (Geyer and Daniilidis, 2001) showed that the paracatadioptric imaging process is equivalent to the following two-step mapping by a sphere (see Fig.1): Firstly, under the viewing sphere coordinate system $O-X_sY_sZ_s$, a 3D point $\mathbf{X} = (x,y,z)^T$ is projected to a point $\mathbf{X_s} = (x_s,y_s,z_s)^T$ on the unit sphere centered at the viewpoint $\mathbf{O}$; Secondly, the point $\mathbf{X_s}$ is projected to a point $\mathbf{m}$ on the image plane Π by a pinhole camera through the perspective center $\mathbf{O^c}$. The image plane is perpendicular to the line going through the viewpoints $\mathbf{O}$ and $\mathbf{O^c}$. Let the intrinsic parameter matrix of the pinhole camera be

$$\mathbf{K}_c = \begin{pmatrix} r_c f_c & s & u_0 \\ 0 & f_c & v_0 \\ 0 & 0 & 1 \end{pmatrix}$$

where r_c is the aspect ratio, f_c is the effective focal length, $(u_0, v_0, 1)^T$ denoted as $\mathbf{p}$ is the principal point, and s is the skew factor.

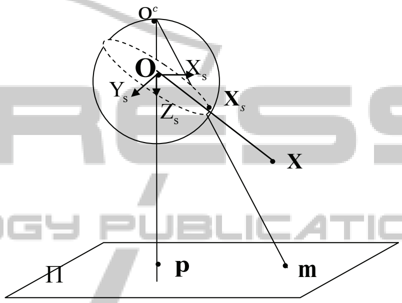

Figure 1: The image formation of a point.

Then, the imaging process of a space point $\mathbf{X}$ to $\mathbf{m}$ can be described as:

$$\alpha \mathbf{m} = \mathbf{K}_c\left(\frac{\mathbf{RX}+\mathbf{t}}{\|\mathbf{RX}+\mathbf{t}\|} + \mathbf{e}\right). \tag{1}$$

where α is a scalar, $\mathbf{R}$ is a 3×3 rotation matrix, $\mathbf{t}$ is a 3-vector of translation, $\|\cdot\|$ denotes the norm of vector in it, $\mathbf{e} = (0,0,1)^T$.

2.2 The Antipodal Image Points

Under paracatadioptric camera, Wu et al. (Wu et al., 2008) gave the definition of antipodal image points and studied their properties as follows:

Definition 1. $\{\mathbf{m}, \mathbf{m}'\}$ is called a pair of antipodal image points if they could be images of two end points of a diameter of the viewing sphere(See Fig.2).

Proposition 1. If $\{\mathbf{m}, \mathbf{m}'\}$ is a pair of antipodal image points under paracatadioptric camera, we have:

$$\frac{1}{\mathbf{m}^T \varpi \mathbf{m}}\mathbf{m} + \frac{1}{\mathbf{m}'^T \varpi \mathbf{m}'}\mathbf{m}' = \mathbf{p}. \tag{2}$$

where $\varpi = \mathbf{K}_c^{-T}\mathbf{K}_c^{-1}$, and $\mathbf{p}$ is the principal point.

2.3 The Paracatadioptric Circle Image

Generally, the projection of a circle is a quartic curve under paracatadioptric camera. Duan and Wu(Duan

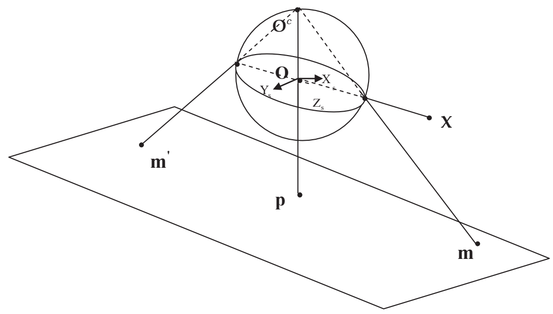

Figure 2: $\{\mathbf{m}, \mathbf{m}^{'}\}$ is a pair of antipodal image points.

and Wu, 2011b) derived the algebraic expression of circle image. In order to make this paper complete, we show the detail as follows.

Firstly, set up the world coordinate system (see Fig.3): $\mathbf{O}$ as the origin $\mathbf{O}_W$; the line through the origin $\mathbf{O}_W$ and orthogonal to the plane containing $\mathbf{c}$ as the $Z-$axis; the point where $Z-$axis and the plane containing $\mathbf{c}$ intersect as the point $\mathbf{o}$, the line through the point $\mathbf{o}$ and center of $\mathbf{c}$ as the line l, then the line through the origin $\mathbf{O}_W$ and parallel to the line l as $X-$axis; the line through the origin $\mathbf{O}_W$ and orthogonal to the $X-$axis and $Z-$axis as $Y-$axis; denoted as $\mathbf{O}_W - X_W, Y_W, Z_W$. Then, under the world coordinate system, the equation of the circle $\mathbf{c}$ is:

$$\begin{cases} (x-x_0)^2 + y^2 = r^2 \\ z = z_0 \end{cases}$$

where z_0 is the distance from the origin $\mathbf{O}_W$ to the plane containing $\mathbf{c}$, r is the radius of $\mathbf{c}$, x_0 is the coordinate of the center of $\mathbf{c}$ under the world coordinate system.

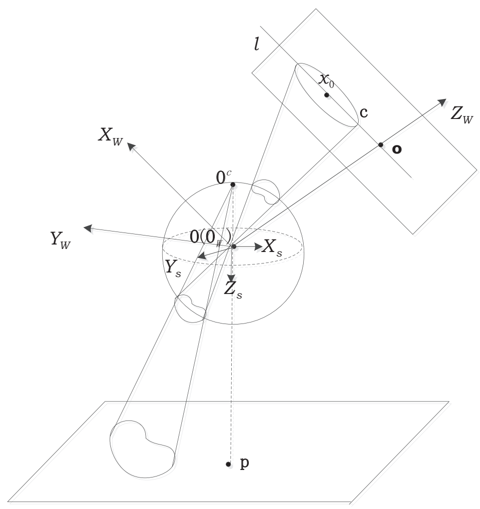

Figure 3: The image formation of a circle.

Proposition 2. Let $\mathbf{m}$ be one image point on paracatadioptric circle image, denote $\widetilde{\mathbf{m}} = \mathbf{K}_c^{-1}\mathbf{m}$. Then, the equation of locus of the point $\mathbf{m}$ is:

$$4\,\widetilde{\mathbf{m}}^T \widehat{\mathbf{C}} \widetilde{\mathbf{m}} - 4\,\widetilde{\mathbf{m}}^T \widehat{\mathbf{C}} \mathbf{e}\,\widetilde{\mathbf{m}}^T \widetilde{\mathbf{m}} + \mathbf{e}^T \widehat{\mathbf{C}} \mathbf{e}\,(\widetilde{\mathbf{m}}^T \widetilde{\mathbf{m}})^2 = 0, \quad (3)$$

where $\mathbf{e} = (0,0,1)^T$, $\widehat{\mathbf{C}} = \mathbf{R}^{-T}\mathbf{C}_1\mathbf{R}^{-1}$, $\mathbf{R}$ is the rotation matrix between $\mathbf{O}_W - X_W, Y_W, Z_W$ and $\mathbf{O} - X_s, Y_s, Z_s$, and $\mathbf{C}_1 = \begin{pmatrix} z_0^2 & 0 & -z_0 x_0 \\ 0 & z_0^2 & 0 \\ -z_0 x_0 & 0 & x_0^2 - r^2 \end{pmatrix}$.

3 PROPERTIES OF PARACATADIOPTRIC CIRCLE IMAGE

Generally, the basic pinhole camera, that is $r_c = 1$ and $s = 0$, is widely used in the real word. In this section, we only study properties of the circle image under basic paracatadioptric camera.

Under paracatadioptric camera, the intrinsic parameter $\mathbf{K}_c$

$$\mathbf{K}_c = \begin{pmatrix} r_c f_c & s & u_0 \\ 0 & f_c & v_0 \\ 0 & 0 & 1 \end{pmatrix},$$

then

$$\mathbf{K}_c^{-1} = \begin{pmatrix} \frac{1}{r_c f_c} & -\frac{s}{r_c f_c^2} & \frac{s v_0}{r_c f_c^2} - \frac{u_0}{r_c f_c} \\ 0 & \frac{1}{f_c} & -\frac{v_0}{f_c} \\ 0 & 0 & 1 \end{pmatrix}.$$

In order to simplify the expressions, we denote

$$\mathbf{K}_c^{-1} = \begin{pmatrix} a & b & d \\ 0 & c & e \\ 0 & 0 & 1 \end{pmatrix}, \hat{\mathbf{C}} = \begin{pmatrix} c_{11} & c_{12} & c_{13} \\ c_{12} & c_{22} & c_{23} \\ c_{13} & c_{23} & c_{33} \end{pmatrix}.$$

Eq(3) shows that the paracatadioptric projection of a circle is a quartic curve. Since a quartic has 14 independent degrees of freedom (DOF), it can also be represented by a point $\mathbf{C}$ in the 14D projective space. Henceforth, we will assume both representations without distinction. Expanding Eq(3) by Maple, we obtain the algebraic expression of paracatadioptric circle image. Let $\mathbf{m} = (x,y,1)^T$ be one point on the circle image, then

$$\hat{\omega}\mathbf{C} = 0,$$

where $\mathbf{C}$ is a 15×1 vector and $\hat{\omega} = (x^4, x^3y, x^2y^2, xy^3, y^4, x^3, x^2y, xy^2, y^3, x^2, xy, y^2, x, y, 1)$. Due to the complexity of circle image $\mathbf{C}$, we only show the first nine terms as follows:

$$\mathbf{C}(1:9)=\begin{pmatrix} a^4c_{33} \\ 4a^3bc_{33} \\ (2a^2c^2+6a^2b^2)c_{33} \\ (4ab^3+4abc^2)c_{33} \\ (2d^2c^2+d^4+c^4)c_{33} \\ 4a^3(c_{13}-dc_{33}) \\ -12a^2b(c_{13}-dc_{33})-4a^2c(c_{23}-ec_{33}) \\ -(12ab^2+4ac^2)(c_{13}-dc_{33})-8abc(c_{23}-ec_{33}) \\ -(4bc^2+4b^3(c_{13}-dc_{33}))-(4c^3+4b^2c)(c_{23}-ec_{33}) \end{pmatrix} \tag{4}$$

Under basic paracatadioptric camera, that is $r_c=1$ and $s=0$, the algebraic expressions of circle image $\mathbf{C}$ changes into
$\mathbf{C}(1:9)=$

$$(a^4c_{33},0,2a^4c_{33},0,a^4c_{33},-4a^3t_1,-4a^3t_2,-4a^3t_1,-4a^3t_2)^T \tag{5}$$

and $\mathbf{C}(10:15)=$

$$\begin{pmatrix} -2a^2(6dt_1+2et_2-2t_3+(d^2+e^2+1)c_{33}) \\ -8a^2(et_1+dt_2-t_5) \\ -2a^2(2dt_1+6et_2-2t_4+(d^2+e^2+1)c_{33}) \\ -4a((3d^2+e^2-1)t_1+2det_2-2dt_3-2et_5) \\ -4a(2det_1+(d^2+3e^2-1)t_2-2et_4-2dt_5) \\ 4(d^2t_3+e^2t_4+2det_5-(d^2+e^2-1))(dt_1+et_2)+(d^2+e^2+1)^2c_{33} \end{pmatrix}, \tag{6}$$

where

$$\begin{cases} t_1=c_{13}-dc_{33}, \\ t_2=c_{23}-ec_{33}, \\ t_3=c_{11}-d^2c_{33}, \\ t_4=c_{22}-e^2c_{33}, \\ t_5=c_{12}-dec_{33}. \end{cases}$$

Generally, the principal point can be correctly estimated through the image center(Alberto et al., 2002) or the projected contour of parabolic mirror. Thus, under basic paracatadioptric camera, assume that the principal point is known, we derive the sufficient and necessary conditions that must be satisfied by circle image.

Theorem 1. Under basic paracatadioptric camera, let the principal point $\mathbf{p}=(u_0,v_0,1)^T$ be known, and $\mathbf{C}$ be the paracatadioptric projection of a circle, then the sufficient and necessary conditions that must be satisfied by $\mathbf{C}$ are as follows:

(a) $\delta_1=\mathbf{C}(3)-2\mathbf{C}(1)=0,$
(b) $\delta_2=\mathbf{C}(5)-\mathbf{C}(1)=0,$
(c) $\delta_3=\mathbf{C}(6)-\mathbf{C}(8)=0,$
(d) $\delta_4=\mathbf{C}(7)-\mathbf{C}(9)=0,$
(e) $\delta_5=\mathbf{C}(2)=\mathbf{C}(4)=0,$
(f) $\delta_6=(\mathbf{C}(7)+4v_0\mathbf{C}(1))\alpha_1-(\mathbf{C}(6)+4u_0\mathbf{C}(1))\alpha_2=0,$
(g) $\delta_7=\mathbf{C}(1)\beta_2^2-(\mathbf{C}(6)+4u_0\mathbf{C}(1))^2\beta_1=0,$
or $\delta_7=\mathbf{C}(1)\beta_3^2-(\mathbf{C}(7)+4v_0\mathbf{C}(1))^2\beta_1=0.$

where

$$\begin{cases} \alpha_1= \\ \mathbf{C}(13)+2u_0v_0\mathbf{C}(7)+2u_0^2\mathbf{C}(6)+2u_0\mathbf{C}(10)+v_0\mathbf{C}(11), \\ \alpha_2= \\ \mathbf{C}(14)+2u_0v_0\mathbf{C}(6)+2v_0^2\mathbf{C}(7)+2v_0\mathbf{C}(12)+u_0\mathbf{C}(11), \end{cases}$$

and

$$\begin{cases} \beta_1=\mathbf{C}(15)+v_0\mathbf{C}(14)+u_0\mathbf{C}(13)+v_0^2\mathbf{C}(12)+u_0v_0 \\ \quad \mathbf{C}(11)+u_0^2\mathbf{C}(10)+(u_0^2+v_0^2)(v_0\mathbf{C}(7)+u_0\mathbf{C}(6) \\ \quad +\mathbf{C}(1)), \\ \beta_2=\mathbf{C}(13)+2u_0\mathbf{C}(10)+v_0\mathbf{C}(11)+(3u_0^2+v_0^2)\mathbf{C}(6) \\ \quad +2u_0v_0\mathbf{C}(7)+4u_0(u_0^2+v_0^2)\mathbf{C}(1), \\ \beta_3=\mathbf{C}(14)+u_0\mathbf{C}(11)+2v_0\mathbf{C}(12)+(u_0^2+3v_0^2)\mathbf{C}(7) \\ \quad +2u_0v_0\mathbf{C}(6)+4v_0(u_0^2+v_0^2)\mathbf{C}(1). \end{cases}$$

Proof. " $\Leftarrow$ " Consider the uncalibrated image of a circle that is mapped in a quartic curve. A quartic curve has 14 DOF. In addition, A circle in 3D gives rise to 6 unknowns (3 for position, 1 for radius, 2 for orientation), which correspond to the matrix $\hat{\mathbf{C}}$ (See Eq(3)). Moreover, the focal length of paracatadioptric camera is also unknown. Thus there are a total of 7 unknowns (DOF). Since $14>7$, then it is obvious that there are sets of quartic curves that can never be the paracatadioptric projection of a circle. The quartic curves that can correspond to the images of circles lie in a subspace of dimension 7. This means that there are 8 independent constraints, which proves the sufficiency of the conditions $\delta_i, i=1,2,\ldots,7$.

" $\Rightarrow$ " From Eq(5), it is obvious that $\delta_1,\delta_2,\delta_3$ and δ_4 are true. In addition, from the second term and the fourth term in Eq(5), we have

$$\mathbf{C}(2)=0,\ \mathbf{C}(4)=0.$$

From the first five terms in Eq(4), we know that

$$\mathbf{C}(4)^2\mathbf{C}(1)-\mathbf{C}(5)\mathbf{C}(2)^2=0.$$

Under basic paracatadioptric camera, $\mathbf{C}(5)-\mathbf{C}(1)=0$, then the above equation changes into

$$\delta_1=\mathbf{C}(2)=\mathbf{C}(4)=0.$$

In the following, we give the proofs of δ_6 and δ_7 in detail.

From $\mathbf{K}_c^{-1}$, we know that

$$\frac{1}{a}=f_c,\frac{d}{a}=-u_0,\frac{e}{a}=-v_0. \tag{7}$$

Generally, $c_{33}\neq 0$ and $a=\frac{1}{f_c}\neq 0$, denote

$$\tau_1=f_c\frac{t_1}{c_{33}},\tau_2=f_c\frac{t_2}{c_{33}},$$

$$\tau_3=f_c^2\frac{t_3}{c_{33}},\tau_4=f_c^2\frac{t_4}{c_{33}},\tau_5=f_c^2\frac{t_5}{c_{33}}.$$

From $\mathbf{C}(6)$ and $\mathbf{C}(7)$ in Eq(5), we have

$$\tau_1=-\frac{1}{4}\frac{\mathbf{C}(6)}{\mathbf{C}(1)},\tau_2=-\frac{1}{4}\frac{\mathbf{C}(7)}{\mathbf{C}(1)}. \tag{8}$$

Moreover, dividing $\mathbf{C}(1)$ from Eq(6) respectively, it follows that

$$\begin{cases} \frac{\mathbf{C}(10)}{\mathbf{C}(1)} = 2(6u_0\tau_1 + 2v_0\tau_2 + 2\tau_3 - (u_0^2 + v_0^2 + f_c^2)), \\ \frac{\mathbf{C}(11)}{\mathbf{C}(1)} = 8(v_0\tau_1 + u_0\tau_2 + \tau_5), \\ \frac{\mathbf{C}(12)}{\mathbf{C}(1)} = 2(2u_0\tau_1 + 6v_0\tau_2 + 2\tau_4 - (u_0^2 + v_0^2 + f_c^2)), \\ \frac{\mathbf{C}(13)}{\mathbf{C}(1)} = -4((3u_0^2 + v_0^2 - f_c^2)\tau_1 + 2u_0v_0\tau_2 + 2u_0\tau_3 + 2v_0\tau_5), \\ \frac{\mathbf{C}(14)}{\mathbf{C}(1)} = -4(2u_0v_0\tau_1 + (u_0^2 + 3v_0^2 - f_c^2)\tau_2 + 2v_0\tau_4 + 2u_0\tau_5), \\ \frac{\mathbf{C}(15)}{\mathbf{C}(1)} = 4((u_0^2 + v_0^2 - f_c^2)(u_0\tau_1 + v_0\tau_2) + u_0^2\tau_3 + v_0^2\tau_4 \\ \qquad +2u_0v_0\tau_5) + (u_0^2 + v_0^2 + f_c^2)^2. \end{cases} \tag{9}$$

Substituting Eq(7) and Eq(8) into the first three terms in Eq(9), then solving for τ_3, τ_4 and τ_5 yields

$$\begin{cases} \tau_3 = \frac{1}{4}(\frac{\mathbf{C}(10)}{\mathbf{C}(1)} + 3u_0\frac{\mathbf{C}(6)}{\mathbf{C}(1)} + v_0\frac{\mathbf{C}(7)}{\mathbf{C}(1)} + 2(u_0^2 + v_0^2 + f_c^2)), \\ \tau_4 = \frac{1}{4}(\frac{\mathbf{C}(12)}{\mathbf{C}(1)} + u_0\frac{\mathbf{C}(6)}{\mathbf{C}(1)} + 3v_0\frac{\mathbf{C}(7)}{\mathbf{C}(1)} + 2(u_0^2 + v_0^2 + f_c^2)), \\ \tau_5 = \frac{1}{8}(\frac{\mathbf{C}(11)}{\mathbf{C}(1)} + 2u_0\frac{\mathbf{C}(7)}{\mathbf{C}(1)} + 2v_0\frac{\mathbf{C}(6)}{\mathbf{C}(1)}). \end{cases} \tag{10}$$

Substituting Eq(8) and Eq(10) into the last three terms in Eq(9), we obtain

$$\begin{gathered} (\mathbf{C}(6) + 4u_0\mathbf{C}(1))f_c^2 + 4u_0(u_0^2 + v_0^2)\mathbf{C}(1) + \mathbf{C}(13) \\ +(3u_0^2 + v_0^2)\mathbf{C}(6) + 2u_0v_0\mathbf{C}(7) + 2u_0\mathbf{C}(10) + v_0\mathbf{C}(11) = 0, \end{gathered} \tag{11}$$

$$\begin{gathered} (\mathbf{C}(7) + 4v_0\mathbf{C}(1))f_c^2 + 4v_0(u_0^2 + v_0^2)\mathbf{C}(1) + \mathbf{C}(14) \\ +(u_0^2 + 3v_0^2)\mathbf{C}(7) + 2u_0v_0\mathbf{C}(6) + u_0\mathbf{C}(11) + 2v_0\mathbf{C}(12) = 0, \end{gathered} \tag{12}$$

$$\begin{gathered} \mathbf{C}(1)f_c^4 + (u_0\mathbf{C}(6) + v_0\mathbf{C}(7) + 4(u_0^2 + v_0^2)\mathbf{C}(1))f_c^2 \\ +3(u_0^2 + v_0^2)^2\mathbf{C}(1) - \mathbf{C}(15) + 2(u_0^2 + v_0^2)(u_0\mathbf{C}(6) + v_0\mathbf{C}(7)) \\ +u_0^2\mathbf{C}(10) + v_0^2\mathbf{C}(12) + u_0v_0\mathbf{C}(11) = 0. \end{gathered} \tag{13}$$

Subtracting $(\mathbf{C}(6) + 4u_0\mathbf{C}(1))\times$ Eq(12) from $(\mathbf{C}(7) + 4v_0\mathbf{C}(1))\times$ Eq(11) follows that

$$\delta_6 = (\mathbf{C}(7) + 4v_0\mathbf{C}(1))\alpha_1 - (\mathbf{C}(6) + 4u_0\mathbf{C}(1))\alpha_2 = 0.$$

What's more, subtracting Eq(13) from $(u_0 \times \text{Eq}(12) + v_0 \times \text{Eq}(12))$ yields

$$\mathbf{C}(1)f_c^4 - \beta_1 = 0, \tag{14}$$

where

$$\begin{gathered} \beta_1 = \mathbf{C}(15) + v_0\mathbf{C}(14) + u_0\mathbf{C}(13) + v_0^2\mathbf{C}(12) + u_0v_0\mathbf{C}(11) \\ +u_0^2\mathbf{C}(10) + (u_0^2 + v_0^2)(v_0\mathbf{C}(7) + u_0\mathbf{C}(6) + \mathbf{C}(1)). \end{gathered}$$

Eliminating f_c^4 from Eq(11) and Eq(14) or from Eq(12) and Eq(14), we have

$$\delta_7 = \mathbf{C}(1)\beta_2^2 - (\mathbf{C}(6) + 4u_0\mathbf{C}(1))^2\beta_1 = 0,$$

or

$$\delta_7 = \mathbf{C}(1)\beta_3^2 - (\mathbf{C}(7) + 4v_0\mathbf{C}(1))^2\beta_1 = 0.$$

where

$$\begin{cases} \beta_2 = \mathbf{C}(13) + 2u_0\mathbf{C}(10) + v_0\mathbf{C}(11) \\ +(3u_0^2 + v_0^2)\mathbf{C}(6) + 2u_0v_0\mathbf{C}(7) + 4u_0(u_0^2 + v_0^2)\mathbf{C}(1), \\ \beta_3 = \mathbf{C}(14) + u_0\mathbf{C}(11) + 2v_0\mathbf{C}(12) \\ +(u_0^2 + 3v_0^2)\mathbf{C}(7) + 2u_0v_0\mathbf{C}(6) + 4v_0(u_0^2 + v_0^2)\mathbf{C}(1). \end{cases}$$

As shown above, $\delta_i, i = 1, 2, ..., 7$ are derived from different coefficients of the circle image equation $\mathbf{C}$, thus these seven conditions on the quartic curve are independent. This completes the proof.

Assume that $\mathbf{C}$ is the projection of a circle under basic paracatadioptric camera, then the sufficient and necessary conditions derived in Theorem 1 can be used to limit the search space to correctly fit the circle image.

4 CALIBRATION OF THE FOCAL LENGTH FROM CIRCLE IMAGE

In this section, we show that the focal length can be calibrated from one circle image and the principal point. At first, the sufficient and necessary conditions in Theorem 1 are used to fit circle image under basic paracatadioptric camera. Then, the focal length can be computed from the estimated circle image.

Let $\mathbf{C}$ be the image of a circle under an uncalibrated paracatadioptric camera and $\mathbf{m}_i$, $i = 1, 2, 3, ..., N$ with $N \geq 7$ be points on $\mathbf{C}$.

4.1 Fitting Paracatadioptric Circle Image

4.1.1 Initialization

Usually, the projected contour of parabolic mirror is visible and a conic, denoted as $\mathbf{C}_0$. At first, by the least square method, we fit this projected contour $\mathbf{C}_0$ and use the result to make some initializations. Assume that the expression of $\mathbf{C}_0$ is:

$$\mathbf{C_0} = \begin{pmatrix} \tilde{a} & \tilde{b} & \tilde{d} \\ \tilde{b} & \tilde{c} & \tilde{e} \\ \tilde{d} & \tilde{e} & \tilde{f} \end{pmatrix},$$

the initial values of r_c, s, u_0, v_0, f_c can be obtained (Ying and Hu, 2004):

$$\begin{cases} r_c = \sqrt{-\frac{\tilde{b}^2}{\tilde{a}^2} + \frac{\tilde{c}}{\tilde{a}}}, \\ s = -\frac{\tilde{b}}{\tilde{a}}, \\ u_0 = \frac{\tilde{b}\tilde{e} - \tilde{c}\tilde{d}}{\tilde{a}\tilde{c} - \tilde{b}^2}, \\ v_0 = \frac{\tilde{b}\tilde{d} - \tilde{a}\tilde{e}}{\tilde{a}\tilde{c} - \tilde{b}^2}, \\ f_c = u_0^2\tilde{a} + 2u_0v_0\tilde{b} + v_0^2\tilde{c} + 2u_0\tilde{d} + 2v_0\tilde{e} + \tilde{f}. \end{cases} \tag{15}$$

Next, compute the antipodal image points $\mathbf{m}_i^{'}$ of $\mathbf{m}_i$ using the obtained intrinsic parameters in (15), $i = 1, 2, 3, ..., N$ by Proposition1. Then, initialize paracatadioptric circle image $\mathbf{C}$ using $\{\mathbf{m}_i, \mathbf{m}_i^{'}, i =$

$1,2,...,N\}$ through minimizing the object function as follows:

$$F_1 = \mathbf{C}^T \mathbf{M}^T \mathbf{M}\mathbf{C}, \tag{16}$$

where $\mathbf{M} = (\hat{\omega}_1, \hat{\omega}_2, ..., \hat{\omega}_N, \hat{\omega}_1^{'}, \hat{\omega}_2^{'}, ..., \hat{\omega}_N^{'})^T$.

In Theorem 1, the first six conditions $\delta_i, i = 1,2,...,6$ on circle image is linear, thus Eq(16) changes into:

$$F_1 = \dot{\mathbf{C}}^T \dot{\mathbf{M}}^T \dot{\mathbf{M}}\dot{\mathbf{C}}, \tag{17}$$

where $\dot{\mathbf{M}} = (\dot{\omega}_1, \dot{\omega}_2, ..., \dot{\omega}_N, \dot{\omega}_1^{'}, \dot{\omega}_2^{'}, ..., \dot{\omega}_N^{'})^T$, $\dot{\mathbf{C}} = (\mathbf{C}(1), \mathbf{C}(6), \mathbf{C}(7), \mathbf{C}(10:15)^T)^T$ and $\dot{\omega}_i = (x_i^4 + 2x_i^2 y_i^2 + y_i^4, x_i^3 + x_i y_i^2, y_i^3 + x_i^2 y_i, x_i^2, x_i y_i, y_i^2, x_i, y_i, 1), i = 1,2,...,N$.

So far, we obtain the initializations of the principal point $\mathbf{p} = (u_0, v_0, 1)^T$ and the quartic curve $\mathbf{C}$. Then, the fitting algorithm for paracatadioptric circle image is given as follows.

4.1.2 The Fitting Algorithm

Input: The image points extracted from the projected contour of parabolic mirror and the circle image respectively.

Step 1. Estimate the contour conic $\mathbf{C}_0$ by the least square method and initialize the camera intrinsic parameters by Eq(15);

Step 2. From the initialization camera parameters and image points on the circle image, initialize the paracatadioptric circle image by minimizing the object function Eq(17);

Step 3. Consider the objection function:

$$F_1 = \dot{\mathbf{C}}^T \dot{\mathbf{M}}_1^T \dot{\mathbf{M}}_1 \dot{\mathbf{C}} + \lambda(\delta_6^2 + \delta_7^2), \tag{18}$$

where $\dot{\mathbf{M}}_1 = (\dot{\omega}_1, \dot{\omega}_2, ..., \dot{\omega}_N)^T$, N is the number of image points extracted from the circle image, λ is the Lagrange multiplier and δ_i $(i = 6,7)$ are shown in Theorem 1.

Step 4. Minimize the object function Eq(18) to estimate the paracatadioptric circle image using Gauss-Newton or Levenberg-Marquardt algorithm.

Output: The paracatadioptric circle image $\mathbf{C}$.

4.2 Calibration of the Focal Length

Generally, the principal point can be accurately estimated by the projected contour of parabolic mirror or image center. In addition, from the proof of the Theorem 1, we find that the focal length f_c can be computed from paracatadioptric circle image $\mathbf{C}$ and principal point $\mathbf{p}$. When $\mathbf{C}(1) \neq 0$, $\mathbf{C}(6) + 4u_0\mathbf{C}(1) \neq 0$ and $\mathbf{C}(7) + 4v_0\mathbf{C}(1) \neq 0$, from Eq(12), Eq(13) and Eq(14), we have

$$f_c^2 = -\frac{\beta_2}{\mathbf{C}(6) + 4u_0\mathbf{C}(1)} = -\frac{\beta_3}{\mathbf{C}(7) + 4v_0\mathbf{C}(1)} = \sqrt{\frac{\beta_1}{\mathbf{C}(1)}}, \tag{19}$$

where β_1, β_2 and β_3 are shown in the proof of Theorem 1. Moreover, from Eq(19), it can be seen that the camera parameters can be estimated from one circle image if the high calibration accuracy is not required. Here, the estimated focal length can be used to evaluate the performance of our fitting algorithm proposed in the following.

5 EXPERIMENTS

In this section, we test the proposed algorithm using the simulated and the real images. The fitting algorithm proposed in Section 4 is used to estimated the paracatadioptric circle image. Then from Eq(19), the computed focal length is used to evaluate the performance of our fitting algorithm.

5.1 Using Simulated Data

The simulated camera has the following intrinsic parameter matrix:

$$\mathbf{K}_c = \begin{pmatrix} 600 & 0 & 500 \\ 0 & 600 & 350 \\ 0 & 0 & 1 \end{pmatrix}$$

where $(500, 350, 1)^T$ is the principal point $\mathbf{p}$ and 600 is the focal length f_c.

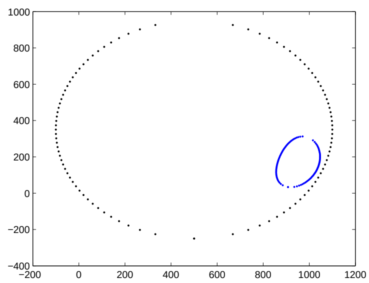

Figure 4: A test image generated by a paracatadioptric camera.

Fig.4 shows a simulated paracatadioptric circle image, where the larger conic is the projected contour of parabolic mirror and the smaller curve is the visible part of circle image. The projected contour and the circle image are consisted of 100 points respectively. Gaussian noise with mean 0 and standard deviation σ ranging from 0 to 3 is directly added to each of the points on the circle image. Because the resolution of the image edge is lower than that of the image center, we add noise with 2σ to the projected contour of parabolic mirror. At each noise level, we perform 100 independent trails respectively.

In the following, we use the algorithm proposed in Section 4 to estimate the paracatadioptric circle image. The mean and standard deviation of the algebraic distance d from points to quartic curve (the circle image) are shown in Fig.5. From Fig.5, it can be seen that paracatadioptric circle can be estimated correctly, which shows the validity of our fitting algorithm.

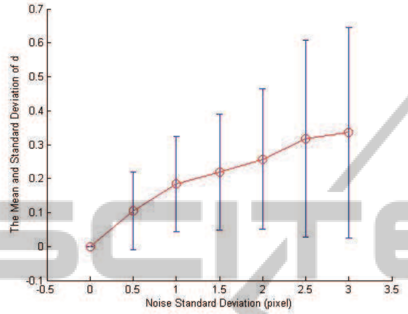

Figure 5: The mean and standard deviation of the distance d from points to circle image.

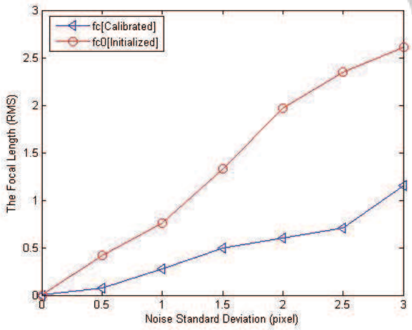

Figure 6: The comparison result of the focal length.

Moreover, the focal length f_c is computed through the estimated paracatadioptric circle image and the initialized principal point from Eq(19). Then, we compare the computed focal length f_c with the initialized focal length f_{c0} in Eq(15). Fig.6 gives the comparison result, which shows that the paracatadioptric circle image can be estimated correctly.

5.2 Using Real Image Data

A real image of two cups is captured by a NIKON COOLPIX990 with a hyperboloid mirror designed by the Center for Machine Perception, Czech technical University. The mirror parameter $\xi = 0.966$ that is close to 1. Here, we approximately regard it as 1. The image of cups is shown in Fig.7(a). Its size is 1080×810 pixels.

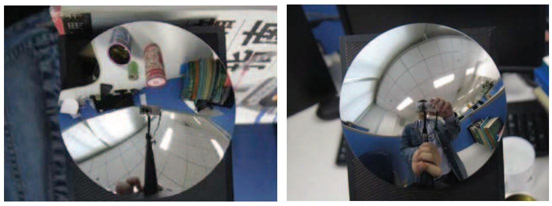

(a) (b)

Figure 7: (a) A real image captured by a paracatadioptric camera. (b) The test image.

Figure 8: The amplified result of estimated paracatadioptric circle image.

The projected contour of mirror and circle images (images of blue cup and red cup) are manually extracted using the software in the website: http//mail.isr.uc.pt/carloss/software/software.htm. Next, applying the fitting algorithm proposed in section 4, images of the two cups can be estimated. To check the fitting result, we reproject the estimated circle images to the original figure (Fig.7(a)). Fig.8 shows the amplified result, and we can see that the circle images can be estimated correctly. In addition, using the estimated circle images and the principal point in Eq(15), the focal length is computed from Eq(19). Then, the computed focal length and the initialized principal point are used to rectify Fig.7(b). Fig.9(a) and Fig.9(b) show the rectified results using the images of two cups respectively. Intuitively, the estimated intrinsic parameters can make those heavy distorted lines become straight, i.e. the proposed fitting method is very effective.

6 CONCLUSIONS

The projection of a circle under paracatadioptric camera is a quartic curve. However, due to the partial occlusion, it is impossible to directly estimate paracatadioptric circle image using image points extracting from the visible part. Consequently, camera parameters cannot be calibrated. In this paper, for the case that aspect ratio is 1 and skew is 0, we study the properties of paracatadioptric circle image and show

(a)

(b)

Figure 9: (a) The rectified result through the image of blue cup, (b) The rectified result through the image of red cup.

that the focal length can be calibrated from one circle image. Firstly, we derive the necessary and sufficient conditions of paracatadioptric circle image. Secondly, these conditions are used to limit the search space to accurately estimate circle image. What's more, we show that the focal length can be computed from the estimated circle image and the principal point that is estimated from the projected contour of parabolic mirror. Both the simulated and real data experiments validate the effectiveness of our method. In our future work, we continue to study the calibration method of central catadioptric camera from circle images.

ACKNOWLEDGEMENTS

This work was supported by National Science and Technology Support Projects of China (No.2012BAH07B01).

REFERENCES

Alberto, R., E.Pedro, and Gines, G. (2002). A note on principal point estimability. In *Proc. International Conf. on Pattern Recognition*, pages 11–15. IEEE Press.

Aliaga, D. (2001). Accurate catadioptric calibration for real-time pose estimation in room-size environments. In *Proc. International Conf. of Computer Vision*, pages 127–134. IEEE CS Press.

Baker, S. and Nayer, S. (1999). A theory of single-viewpoint catadioptric image formation. *Int. J. Comput. Vision*, 35:175–196.

Barreto, J. and Araujo, H. (2002). Geometry properties of central catadioptric line images. In *Proc. European Conf. of Computer Vision*, pages 237–251.

Barreto, J. and Araujo, H. (2003). Paracatioptric camera calibration using lines. In *Proc. International Conf. of Computer Vision*. IEEE CS Press.

Barreto, J. and Araujo, H. (2005). Geometry properties of central catadioptric line images and application in calibration. *IEEE Trans. Pattern Anal. Machine Intell.*, 27:1327–1333.

Barreto, J. and Araujo, H. (2006). Fitting conics to paracatadioptric projection of lines. *Computer Vision and Image Understanding*, 101:151–165.

Bastanlar, Y., Puig, L., Sturm, P., and Barreto, J. (2008). Dlt-like calibration of central catadioptric cameras. In *Proc. Workshop on Omnidirectional Vision, Camera Networks and Non-Classical Cameras*.

Deng, X., Wu, F., and Wu, Y. (2007). An easy calibration method for central catadioptric cameras. *Acta Automatica Sinica*, 33:801–808.

Duan, F., Wu, F., Zhou, M., Deng, X., and Tian, Y. (2012). Calibrating effective focal length for central catadioptric cameras using one space line. *Pattern Recognition Letters*, 33:646–653.

Duan, H. and Wu, Y. (2011a). Paracatadioptric camera calibration using sphere images. In *Proc. International Conf. on Image Processing*, pages 649–652. IEEE Press.

Duan, H. and Wu, Y. (2011b). Unified imaging of geometric entities under catadioptric camera and camera calibration. *Journal of Computer-Aided Design and Computer Graphics*, 23:891–898.

Duan, H. and Wu, Y. (2012). A calibration method for paracatadioptric camera from sphere images. *Pattern Recognition Letters*, 33:677–684.

Geyer, C. and Daniilidis, K. (1999). Catadioptric camera calibration. In *Proc. International Conf. of Computer Vision*, pages 398–404. IEEE CS Press.

Geyer, C. and Daniilidis, K. (2001). Catadioptric projective geometry. *Int. J. Comput. Vision*, 45:223–243.

Geyer, C. and Daniilidis, K. (2002). Paracatadioptric camera calibration. *IEEE Trans. Pattern Anal. Machine Intell.*, 24:687–695.

Kang, S. (2000). Catadioptric self-calibration. In *Proc. IEEE Conf. on Computer Vision and Pattern Recognition*, volume 1, pages 201–207.

Scaramuzza, D., Martinelli, A., and Siegwart, R. (2006). A flexible technique for accurate omnidirectional camera calibration and structure from motion. In *Proc. International Conf. of Computer Vision*, pages 45–52. IEEE CS Press.

Sturm, P. and Barreto, J. (2008). General imaging geometry for central catadioptric cameras. In *Proc. European Conf. of Computer Vision*, pages 609–622.

Wu, F., Duan, F., Hu, Z., and Wu, Y. (2008). A new linear algorithm for calibrating central catadioptric cameras. *Pattern Recognition*, 41:3166–3172.

Wu, Y. and Hu, Z. (2005). Geometric invariants and applications under catadioptric camera model. In *Proc. International Conf. of Computer Vision*, pages 1547–1554. IEEE CS Press.

Wu, Y., Li, Y., and Hu, Z. (2006). Easy calibration for paracatadioptric-like camera. In *Proc. International Conf. on Intelligent Robots and Systems*, pages 5719–5724. IEEE Press.

Ying, X. and Hu, Z. (2004). Catadioptric camera calibration using geometric invariants. *IEEE Trans. Pattern Anal. Machine Intell.*, 26:1260–1271.

Ying, X. and Zha, H. (2008). Identical projective geometric properties of central catadioptric lines images and sphere images with applications to calibration. *Int. J. Comput. Vision*, 78:89–105.